A new method for the determination of flow directions and upslope areas in grid digital elevation models

David G. Tarboton

Utah Water Research Laboratory, Utah State University, Logan

Abstract. A new procedure for the representation of flow directions and calculation of upslope areas using rectangular grid digital elevation models is presented. The procedure is based on representing flow direction as a single angle taken as the steepest downward slope on the eight triangular facets centered at each grid point. Upslope area is then calculated by proportioning flow between two downslope pixels according to how close this flow direction is to the direct angle to the downslope pixel. This procedure offers improvements over prior procedures that have restricted flow to eight possible directions (introducing grid bias) or proportioned flow according to slope (introducing unrealistic dispersion). The new procedure is more robust than prior procedures based on fitting local planes while retaining a simple grid based structure. Detailed algorithms are presented and results are demonstrated through test examples and application to digital elevation data sets.

Introduction

Flow directions based on digital elevation models (DEMs) are needed in hydrology to determine the paths of water, sediment, and contaminant movement. Two important distributed quantities that depend on flow directions are the upslope area and specific catchment area. Upslope area, A, is defined as the total catchment area above a point or short length of contour [*Moore et al.*, 1991]. The specific catchment area, a, is defined as the upslope area per unit width of contour, L, ($a = A/L$) [*Moore et al.*, 1991] and is a distributed quantity that has important hydrological, geomorphological, and geological significance [*Costa-Cabral and Burges*, 1994]. The specific catchment area contributing to flow at any particular location is useful for determining relative saturation and generation of runoff from saturation excess in models such as TOPMODEL [*Beven and Kirkby*, 1979; *Beven et al.*, 1984; *Wood et al.*, 1990]. Specific catchment area together with other topographic parameters has also been used in the analysis of processes such as erosion and landslides [*Dietrich et al.*, 1992, 1993; *Wu*, 1993; *Montgomery and Dietrich*, 1994]. Upslope area is commonly used for the automatic demarcation of channels relying on the notion of a critical support area [*O'Callaghan and Mark*, 1984; *Jenson and Domingue*, 1988; *Morris and Heerdegen*, 1988; *Tarboton*, 1989; *Lammers and Band*, 1990; *Tarboton et al.*, 1991, 1992; *Martz and Garbrecht*, 1992]. Judging by the number of recent papers, there is considerable hydrologic interest in the effect of grid scale and procedures for computation of specific catchment area [*Zhang and Montgomery*, 1994; *Quinn et al.*, 1995; *Wolock and McCabe*, 1995]. It is therefore important that flow directions and specific catchment areas be accurately determined free from grid artifacts.

In this paper a new method for calculating flow directions, upslope, and specific catchment areas is presented. In what follows I first review the currently available procedures for calculating upslope and specific catchment areas on the basis

of grid digital elevation models, pointing out their strengths and weaknesses and giving the motivation for a new method. I then describe the new procedure for calculation of flow directions and the procedure for calculation of upslope area on the basis of the new flow directions. Illustrative examples are used to compare the new method with existing methods. These include simple test cases, where the theoretical result is known and bias and square error can be evaluated, as well as low- and high-resolution DEM data where the evaluation is qualitative. Readers familiar with the issues surrounding the computation of upslope area based on grid DEMs could skip the background section.

Background

Grid DEMs consist of a matrix data structure with the topographic elevation of each pixel stored in a matrix node. Grid DEMs are distinct from other DEM representations such as triangular irregular network (TIN) and contour-based data storage structures. Grid DEMs are readily available and simple to use and hence have seen widespread application to the analysis of hydrologic problems [*Moore et al.*, 1991]. However, they suffer from some drawbacks that arise from their grided nature.

The earliest and simplest method for specifying flow directions is to assign flow from each pixel to one of its eight neighbors, either adjacent or diagonal, in the direction with steepest downward slope. This method, designated D8 (eight flow directions), was introduced by *O'Callaghan and Mark* [1984] and has been widely used [*Marks et al.*, 1984; *Band*, 1986; *Jenson and Domingue*, 1988; *Mark*, 1988; *Morris and Heerdegen*, 1988; *Tarboton et al.*, 1988; *Tarboton*, 1989; *Jenson*, 1991; *Martz and Garbrecht*, 1992]. In the context of a grid the upslope area, A, is the area contributing to each pixel and may be estimated as the product of the number of pixels draining through each pixel and pixel area. The specific catchment area, a, is then estimated as A/L, taking L as the pixel width.

The D8 approach has disadvantages arising from the discretization of flow into only one of eight possible directions, separated by 45° [e.g., *Fairfield and Leymarie*, 1991; *Quinn et*
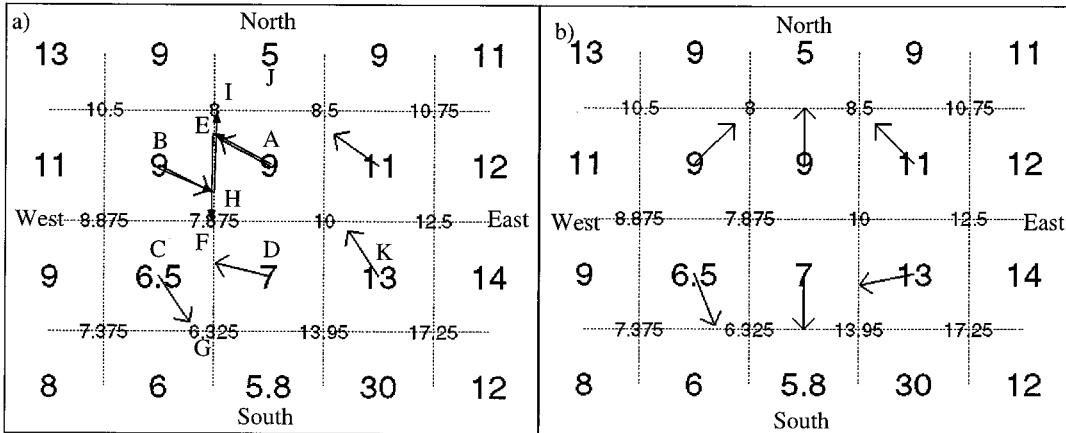
Figure 1. Hypothetical DEM subset on a block-centered grid. Corner elevations are calculated by averaging the elevations of adjoining cells. (a) Flow directions determined using locally fitted planes [*Lea*, 1992]. (b) Flow directions by this papers new procedure. In Figure 1a consider flow from the pixel with center marked A. The pixel immediately to the north is the lowest neighbor, with elevation 5, so that is where water from this pixel should flow. Some water from pixel A should also flow to the south or south west, since pixel A is a saddle. Lea's method has water flow to the northwest along the direction of the plane slope to point E, where it crosses into pixel B. The edge between pixels A and B is a discontinuous edge with flow from the adjacent pixels in opposing directions, a situation that poses problems for plane flow algorithms. Flow from A is routed south along the edge from E to F, where it crosses into pixel C and without exception checking gets stuck in an infinite loop, moving from pixel C to D to A to B around the point F. Furthermore the flow originating at the center of pixel B goes south east to point H, where it enters pixel A and then flows north along the edge (since the slope vector centered at A has a north component), to point I, in an uphill direction, where it enters the pixel J. Thus flows from B and A move in opposite directions along the same edge, an unrealistic situation. Another problem is evident at pixel K. Here flow has a large north component due to the elevation 30 to the south, despite the fact that its lowest neighbor is to the southeast, and neighbor with steepest slope is to the east.

al., 1991; *Costa-Cabral and Burges*, 1994]. *Fairfield and Leymarie* [1991] suggested overcoming these problems by randomly assigning a flow direction to one of the downslope neighbors, with the probability proportional to slope.

Multiple flow direction methods [*Quinn et al.*, 1991; *Freeman*, 1991] have also been suggested as an attempt to solve the limitations of D8. These allocate flow fractionally to each lower neighbor in proportion to the slope (or in the case of Freeman's method, slope to an exponent) toward that neighbor. Multiple flow direction methods, designated here by MS (multiple directions based on slope), have the disadvantage that flow from a pixel is dispersed to all neighboring pixels with lower elevation.

Dispersion is inherent in any method (including the one I describe below) that assigns flow from one pixel to more than one downslope neighbor and manifests itself in terms of spreading of flow from a single pixel. It could be argued that this does not matter because the models that use *a* may use it as a surrogate for a physical quantity that is affected by dispersion. However, dispersion is inconsistent with the physical definition of upslope area, A, and specific catchment area, a. It is important, to the extent possible, to minimize dispersion in the calculation of a. Then, if necessary, physical dispersion can be modeled separately.

Lea [1992] developed an algorithm that uses the aspect associated with each pixel to specify flow directions. Flow is routed as though it were a ball rolling on a plane released from the center of each grid cell. A plane is fit to the elevations of pixel corners, these corner elevations being estimated by averaging the elevations of adjoining pixel center elevations. This procedure has the advantage of specifying flow direction con-

tinuously (as an angle between 0 and 2π) and without dispersion. *Costa-Cabral and Burges* [1994] presented an elaborate set of procedures, named DEMON (digital elevation model networks), that extends the ideas of *Lea* [1992]. Grid elevation values are used as pixel corners, rather than block centered, and a plane surface is fitted for each pixel. *Costa-Cabral and Burges* [1994] recognized flow as two-dimensional originating uniformly over the pixel area, rather than tracking flow paths from the center point of each pixel. They evaluate upslope area through the construction of detailed flow tubes.

The assumption of a plane fit locally to each pixel requires approximation because only three points are required to determine a plane. The best fit plane cannot in general pass through the four corner elevations, leading to a discontinuous representation of the surface at pixel edges. Planes fit locally to certain elevation combinations can lead to inconsistent or counterintuitive flow directions that are a problem in both *Lea*'s [1992] method and in DEMON. Figure 1 illustrates some of these problems. These problems illustrated in the context of Lea's method are also present in DEMON, since the same plane flow directions would arise given the corner elevations shown in Figure 1. The coding of approaches based on fitting local planes, such as Lea's method and DEMON, so that they are robust and work for all possible elevation combinations that may arise in real data is difficult. There are many exceptions, such as the one illustrated in Figure 1, that need to be anticipated and special code developed to account for them. In fact, the code for DEMON upslope [*Costa-Cabral and Burges*, 1994] is unavailable because it is "hard to program and full of special cases" (M. Costa-Cabral, personal communication, 1995).
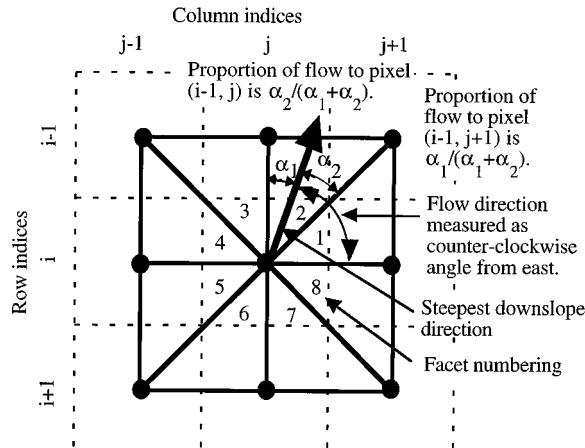
Figure 2. Flow direction defined as steepest downward slope on planar triangular facets on a block-centered grid.

Figure 3. Definition of variables for the calculation of slope on a single facet.

The motivation for developing a new method stemmed from frustration with the way these existing procedures worked. The following issues are relevant to the evaluation and design of DEM flow direction procedures: (1) the need to avoid or minimize dispersion; (2) the need to avoid grid bias, due to the orientation of the numerical grid; (3) the precision with which flow directions are resolved; (4) a simple and efficient grid based matrix storage structure; and (5) robustness, the ability to cope with "difficult" data, such as the saddle in Figure 1 but also with pits and flat areas.

The D8 method does well on points 1, 4, and 5 but resolves flow directions too coarsely (point 3), introducing grid bias (point 2). The randomness in the method of *Fairfield and Leymarie* [1991] is not appealing. Upslope and specific catchment areas are deterministic quantities that we should be able to compute in a repeatable way. The MS method avoids grid bias (point 2) but introduces substantial dispersion. Since flow may be proportioned in up to eight possible directions, eight numbers need to be stored (or recalculated each time they are needed) for each pixel, resulting in inefficient data storage (point 4). The plane flow methods [*Lea*, 1992; *Costa-Cabral and Burges*, 1994] are appealing in that they are deterministic and precisely resolve flow directions. However, they are susceptible to problems (point 5) arising from the approximation involved in fitting a plane through four points.

Calculation of Flow Directions

Here I propose a new method for the representation and calculation of flow directions that is a compromise on the issues raised in the previous section. It recognizes the advantages of *Lea*'s [1992] method and DEMON through the assignment of a single flow direction to each cell. This single flow direction (represented as a continuous quantity between 0 and
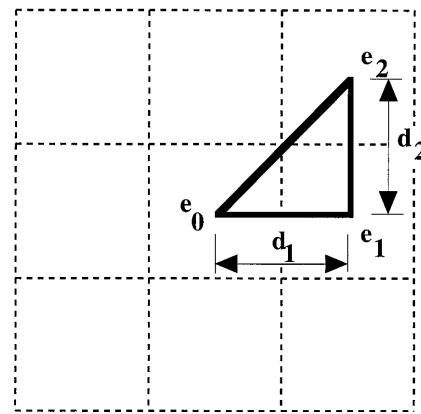
2π) is determined in the direction of the steepest downwards slope on the eight triangular facets formed in a 3×3 pixel window centered on the pixel of interest. The use of triangular facets avoids the approximation involved in fitting a plane and the influence of higher neighbors on downslope flow. Where the direction does not follow one of the cardinal (0, $\pi/2$, π, and $3\pi/2$) or diagonal ($\pi/4$, $3\pi/4$, $5\pi/4$, and $7\pi/4$) directions, upslope area is calculated by apportioning the flow from a pixel between the two downslope pixels according to how close the flow angle is to the direct angle to that pixel center. Since only a single number need be saved for each pixel to represent the flow field, computer storage is simple and efficient. Some dispersion is introduced by the proportioning of flow between downslope pixels, but this is minimized since flow is never proportioned between more than two downslope pixels.

Figure 2 illustrates the calculation of flow directions. A block-centered representation is used with each elevation value taken to represent the elevation of the center of the corresponding pixel. Eight planar triangular facets are formed between the pixel and its eight neighbors. Each of these has a downslope vector which when drawn outward from the center may be at an angle that lies within or outside the 45° ($\pi/4$ radian) angle range of the facet at the center point. If the slope vector angle is within the facet angle, it represents the steepest flow direction on that facet. If the slope vector angle is outside a facet, the steepest flow direction associated with that facet is taken along the steepest edge. The flow direction associated with the pixel is taken as the direction of the steepest downslope vector from all eight facets.

To implement this procedure first consider a single triangular facet (Figure 3). Slope (downward) is represented by the vector (s_1, s_2) where

$$s_1 = (e_0 - e_1)/d_1 \tag{1}$$

$$s_2 = (e_1 - e_2)/d_2 \tag{2}$$

Table 1. Facet Elevation and Factors for Slope and Angle Calculations

Facet	1	2	3	4	5	6	7	8
e_0	$e_{i,j}$	$e_{i,j}$	$e_{i,j}$	$e_{i,j}$	$e_{i,j}$	$e_{i,j}$	$e_{i,j}$	$e_{i,j}$
e_1	$e_{i,j+1}$	$e_{i-1,j}$	$e_{i-1,j}$	$e_{i,j-1}$	$e_{i,j-1}$	$e_{i+1,j}$	$e_{i+1,j}$	$e_{i,j+1}$
e_2	$e_{i-1,j+1}$	$e_{i-1,j+1}$	$e_{i-1,j-1}$	$e_{i-1,j-1}$	$e_{i+1,j-1}$	$e_{i+1,j-1}$	$e_{i+1,j+1}$	$e_{i+1,j+1}$
a_c	0	1	1	2	2	3	3	4
a_f	1	-1	1	-1	1	-1	1	-1

A. Theoretical.   B. D8.

C. MS.   D. Lea's method

E. DEMON   F. D∞
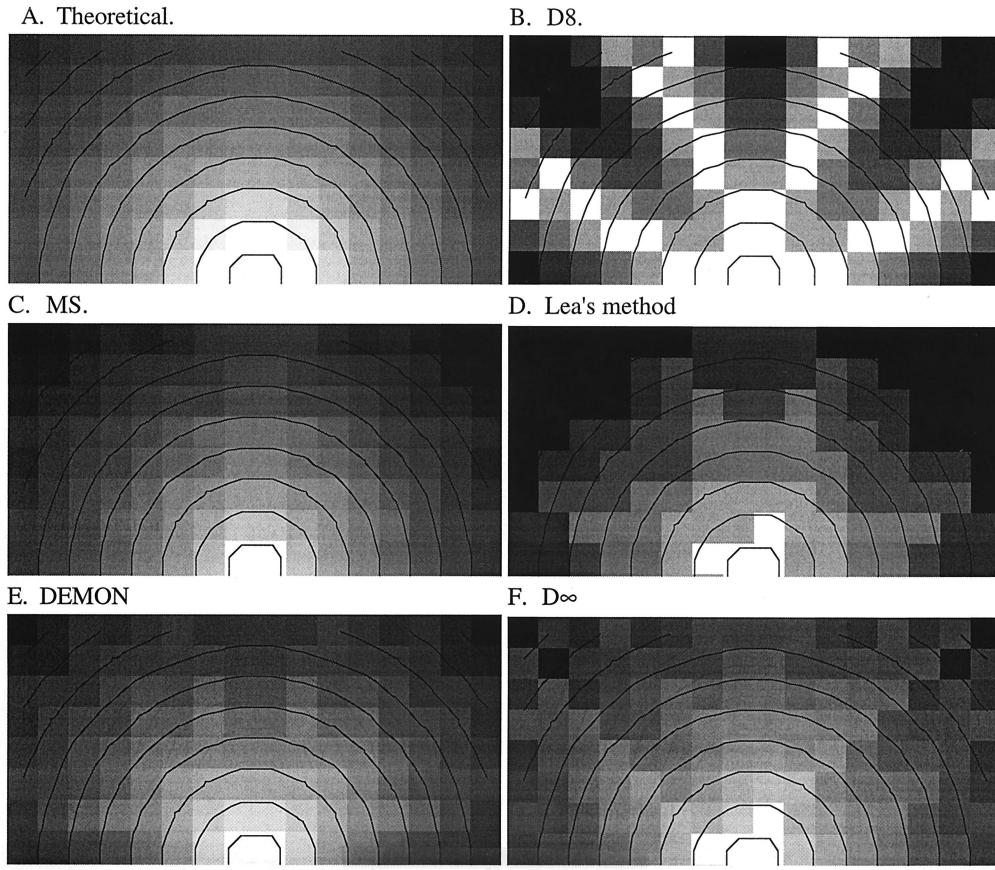
Figure 4. Top half of an outward draining circular cone. Elevation was defined as 200 minus the radius from the center on a 16 × 16 grid with grid spacing 10 units. Specific catchment area is theoretically radius/20 ranging from 0 at the center to 53 on the corners. Contours (10-unit interval) depict elevation. Gray scale depicts contributing area (1 white to 60 black). (a) Theoretical values, (b) single direction (D8) procedure, (c) *Quinn et al.*'s [1991] procedure (MS), (d) *Lea*'s [1992] method, (e) DEMON [*Costa-Cabral and Burges*, 1994], and (f) new procedure (D∞).

and e_i and d_i are elevations and distances between pixels as labeled in Figure 3. The slope direction and magnitude are

$$r = \tan^{-1}(s_2/s_1)$$
$$s = (s_1^2 + s_2^2)^{1/2} \tag{3}$$

If r is not in the range $(0, \tan^{-1}(d_2/d_1))$, then r needs to be set as the direction along the appropriate edge and s assigned as the slope along that edge.

$$\text{if } r < 0, \qquad r = 0, \qquad s = s_1 \tag{4}$$

$$\text{if } r > \tan^{-1}(d_2/d_1), \qquad r = \tan^{-1}(d_2/d_1),$$
$$s = (e_0 - e_2)/(d_1^2 + d_2^2)^{1/2} \tag{5}$$

Next recognize that each of the eight facets depicted in Figure 2 can be mapped by appropriate selection of corner elevations and rotation/transformation onto the facet in Figure 3. Table 1 gives the node elevations corresponding to the corners of each of the triangular facets used to calculate slopes and angles in (1)–(5). These are arranged such that e_0 is the center point, e_1 is the point to the side, and e_2 is the diagonal point. The local angle associated with the largest downwards slope from the eight facets ($r' = r$ from facet with maximum s) is then adjusted to reflect an angle counterclockwise from east (Figure 2) to obtain the flow direction angle.

$$r_g = a_f r' + a_c \pi/2 \tag{6}$$

The multiplier a_f and constant a_c depend on the facet selected and are listed in Table 1. The procedure that searches for the facet with the largest slope proceeds in the order of facets 1 to 8 shown in Figure 1 and in the case of ties (facets with equal slope) picks the first one. In nature ties are extremely rare so the bias introduced by this is deemed negligible.

In the case where no slope vectors are positive (downslope) a flow direction angle of −1 is used to flag the pixel as "unresolved," that is, a flat area or pit. Unresolved flow directions are resolved iteratively by making them flow toward a neighbor of equal elevation that has a flow direction resolved. This is the same approach for resolving pits and flats as used in the D8 method [e.g., *Mark*, 1988; *Jenson and Domingue*, 1988]. I therefore use the calculation of D8 flow directions as a preprocessor to raise the elevation of all pixels in a pit to the level of the overflow. Then where pixels are flagged as "unresolved," the flow angle returned by the D8 procedure is used. This ensures that flat pixels drain to a neighbor that ultimately drains to a lower elevation, eliminating the possibility of inconsistencies such as loops in the flow direction angles. This method of representing flow directions based on triangular facets is designated D∞ (an infinite number of possible single flow directions).

A. Single direction procedure, D8 B. Quinn et al. (1991) procedure, MS C. Lea's (1992) method

D. DEMON   E. New Procedure, D∞
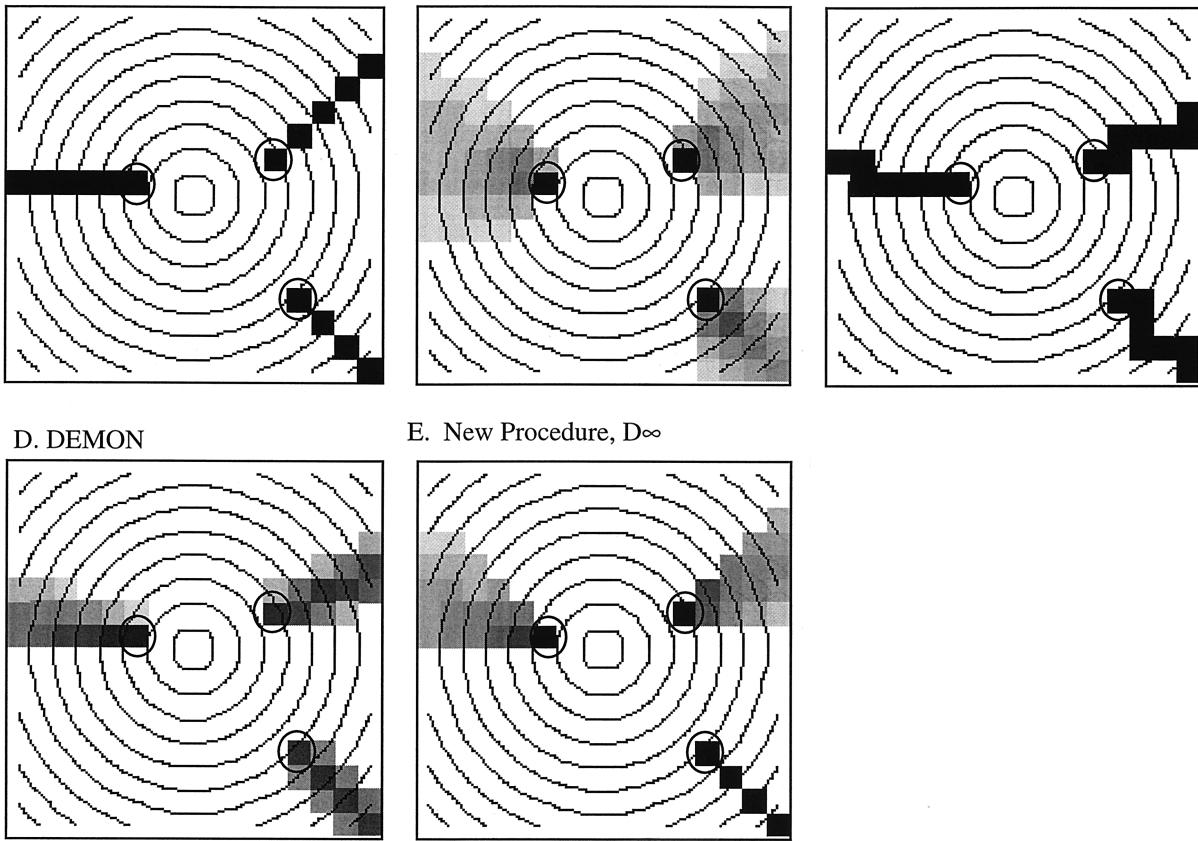
Figure 5. Circular cone influence maps for the circled pixels. Gray scale ranges from white (0 or no influence) to black (1 or 100% influence).

Calculation of Upslope Areas

Upslope area is calculated using a recursive procedure that is an extension of the very efficient recursive algorithm for single directions [*Mark*, 1988]. The upslope area of each pixel is taken as its own area (one) plus the area of upslope neighbors that have some fraction draining to the pixel in question. The flow from each cell either all drains to one neighbor (if the angle falls along a cardinal or diagonal direction) or is on an angle falling between the direct angle to two adjacent neighbors. In the latter case the flow is proportioned between these two neighbor pixels according to how close the flow direction angle is to the direct angle to those pixels. The following pseudocode gives the logic of this algorithm:

Procedure DPAREA(i, j)
  if AREA(i, j) is known
    then
      no action
    else
      AREA(i, j) = 1 (the area of a single pixel)
      for each neighbor (location in, jn)
        p = proportion of neighbor (in, jn) that drains to pixel (i, j) based on angle
        if ($p > 0$) then
          call DPAREA(in, jn) (this is the recursive call to calculate area for the neighbor)
          AREA(i, j) = AREA(i, j) + $p \times$ AREA(in, jn)
Return

The calculation is initiated by calling this function for the outlet pixel. It then recursively calls itself for all pixels that contribute to the upslope area at the outlet. The recursion stops when it reaches a pixel that has no pixels upslope.

Illustrative Examples

This section gives examples of results from this method, D∞, compared to the single direction approach, D8; *Quinn et al.*'s [1991] multidirection algorithm, MS; *Lea*'s [1992] method; and DEMON [*Costa-Cabral and Burges*, 1994]. In these examples we use the notion of influence and dependence maps. The influence function $I(x, x_0)$ is defined as the upslope area at each pixel x from a specific pixel x_0. It maps where flow from pixel x_0 goes and how it is dispersed. It is computed by running a modified version of the procedure for calculating upslope area that uses an area contribution of one from pixel x_0 but zero for all other pixels. The dependence function $D(x, x_0)$ is the opposite of the influence function, defined as $D(x, x_0) = I(x_0, x)$. The upslope area at pixel x_0 is composed of the sum of the area of upslope pixels that have some proportion of their flow go through pixel x_0. $D(x, x_0)$ maps the contribution from pixel x to the calculation of upslope area at x_0. It is calculated through repeated evaluation of the influence function.

Figure 4 shows the upslope area by each approach for a circular cone. Figure 5 shows the influence maps from each of the five algorithms (D8, MS, *Lea*'s [1992] method, DEMON, and D∞) applied to the circular cone. D8 results in no spreading, but flow paths (which are what the influence map plots)
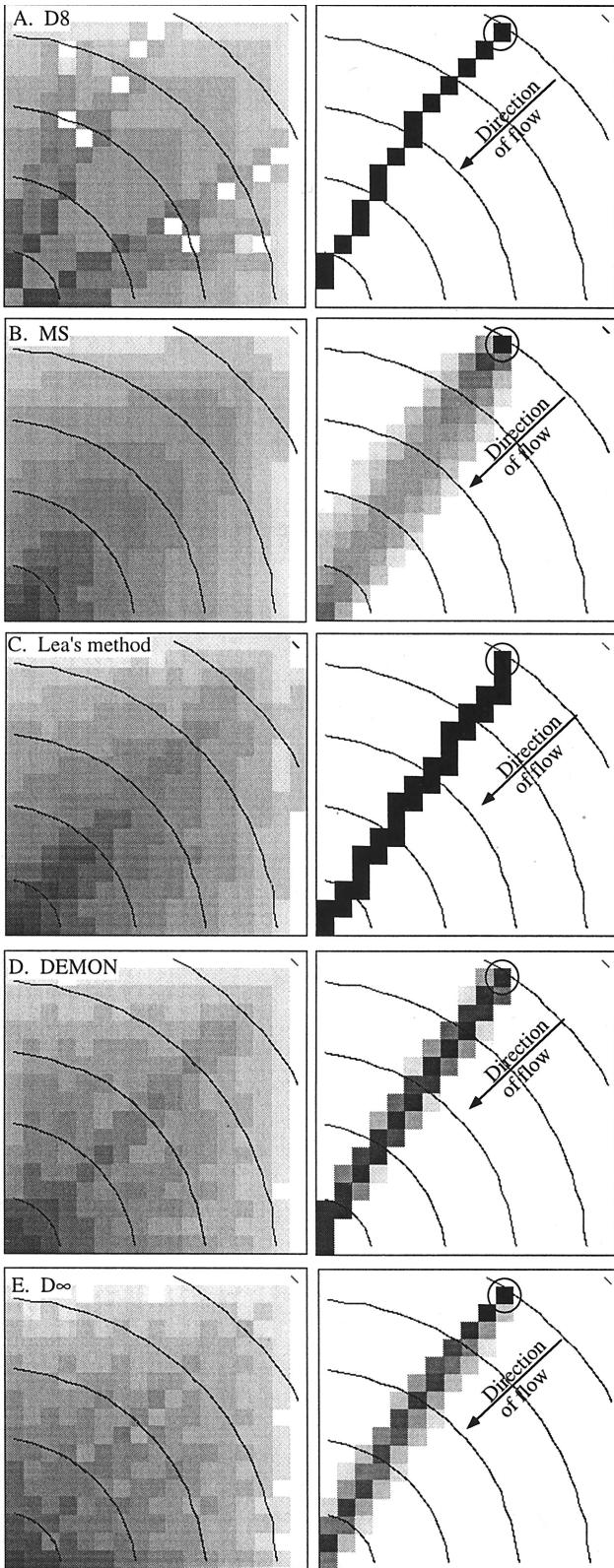
Figure 6. Inward cone. Contours show elevation. The left panels show upslope area in gray scale. The right panels show the influence function from the circled pixel. (a) D8 method, (b) MS method [*Quinn et al.*, 1991], (c) *Lea*'s [1992] method, (d) DEMON [*Costa-Cabral and Burges*, 1994], and (e) D∞ method.

are constrained to grid directions. MS follows the topographic slope but introduces substantial dispersion. *Lea*'s [1992] method marches down the contours in stair step fashion, while DEMON and D∞ strike a balance with spreading slightly wider than divergence perpendicular to the contours. For some pixels (e.g., the lower right one in Figure 5e) D∞ results in no spreading. This is a pixel where the flow direction is aligned with the grid diagonal. In general, when the topographic slope is
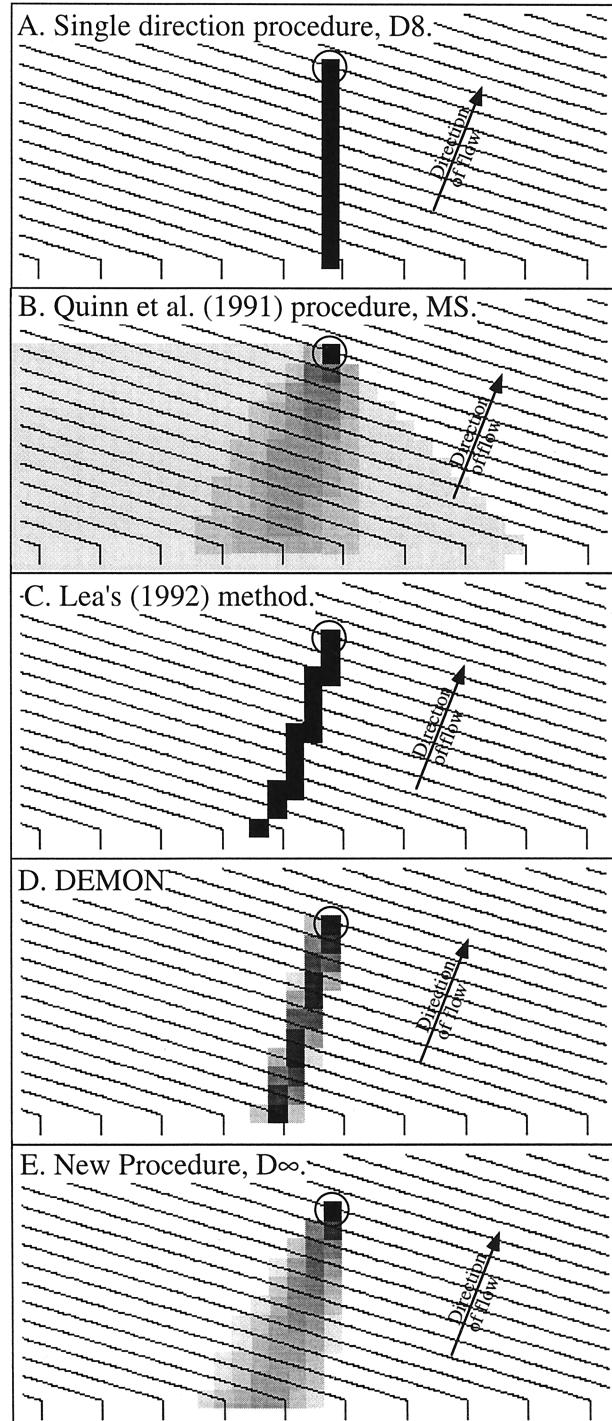
Figure 7. Dependence maps for planar surface. Gray scale (0 white, 1 black) indicates the fraction of each pixel upslope to the circled pixel.
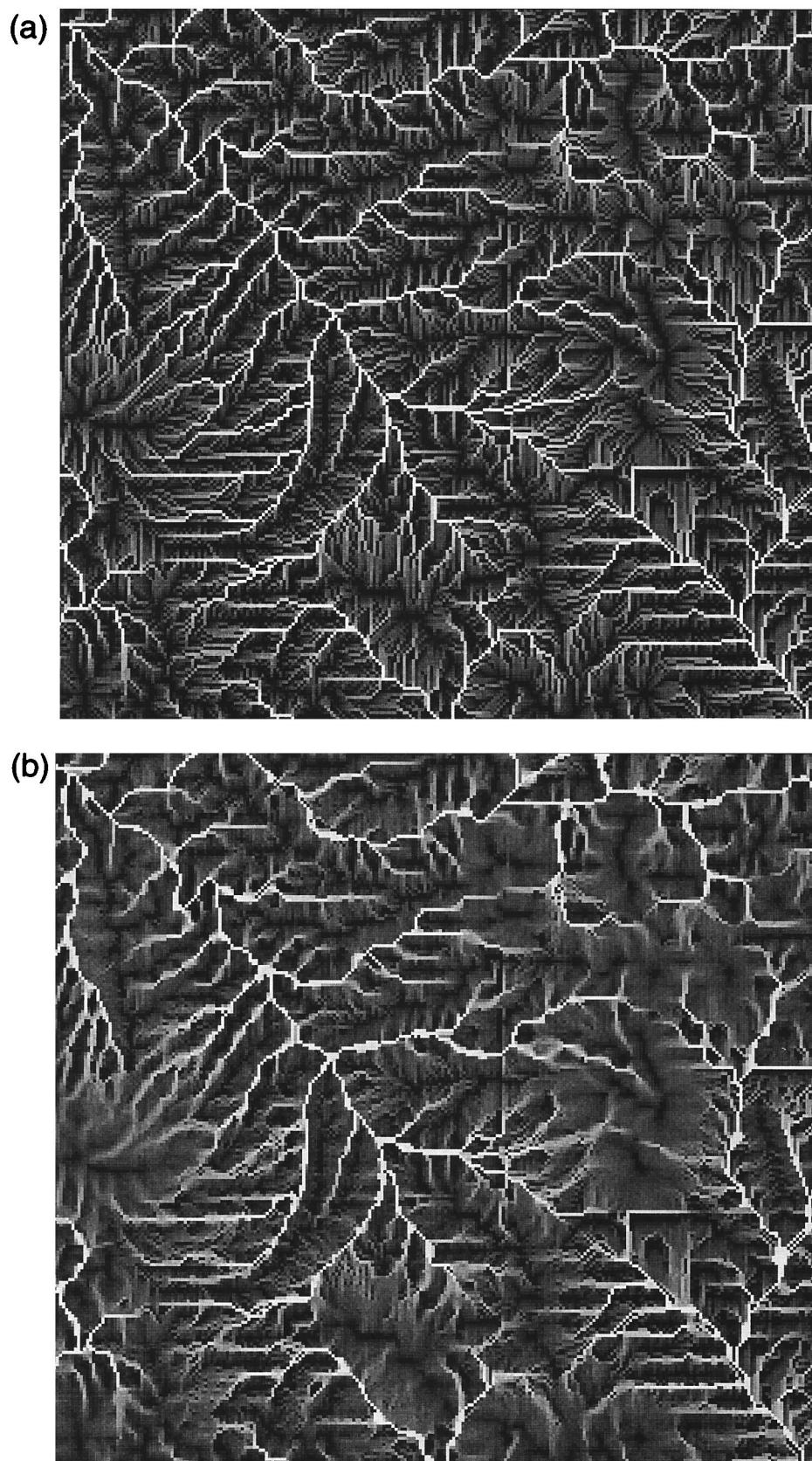
Figure 8. Images of upslope area for a portion of the Walnut Gulch Experimental Watershed DEM. A logarithmic scale of gray shades is used with lighter shades corresponding to higher values. This is a U.S. Geological Survey DEM with 30-m resolution. (a) Single-direction, D8, procedure; (b) *Quinn et al*. [1991] procedure, MS; and (c) new procedure, D∞.
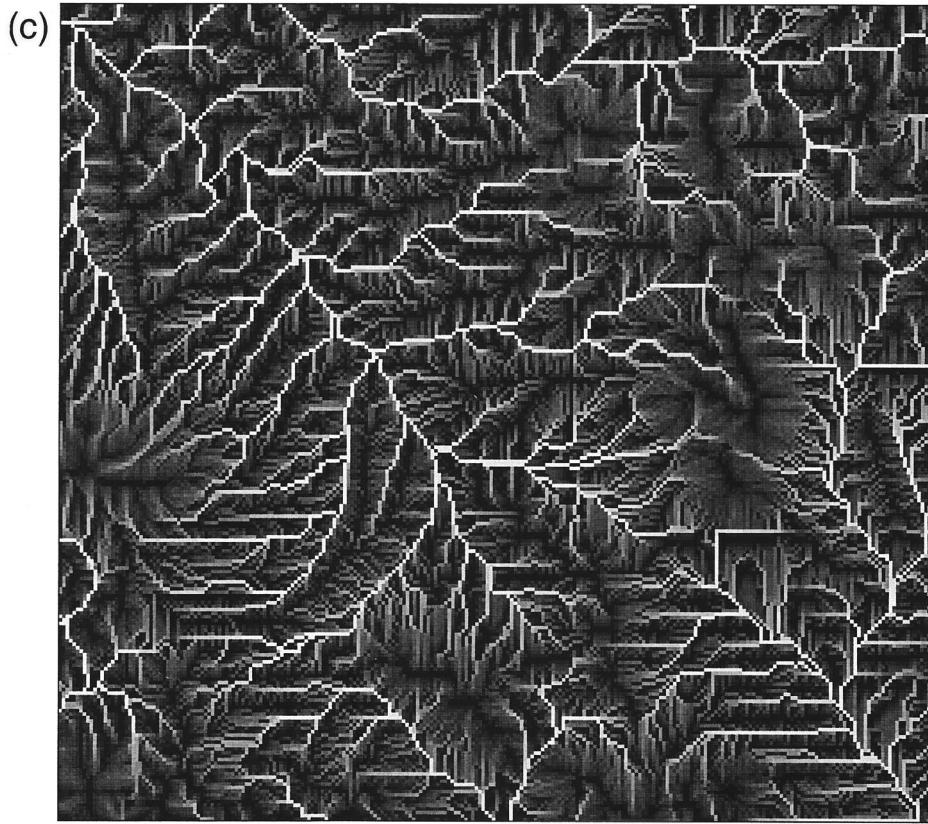
Figure 8. (continued)

aligned with the grid axes, cardinal or diagonal, the D∞ procedure gives the same results as D8, and both are correct. However, when the topographic slope is not aligned with one of the grid directions, the procedures differ. D8 introduces no dispersion, but at the expense of grid bias. D∞ follows the topographic slope at the cost of introducing some dispersion.

Figure 6 shows upslope area and the influence functions for a portion of an inward flowing cone surface. Figure 7 shows the dependence maps for a plane surface not aligned with the grid. The dependence map reflects the fraction of a pixel's area that drains to the designated pixel. It serves to demarcate a zone of contribution, with shading to denote the degree of contribution. On a planar surface the dependence maps should be straight lines perpendicular to the gradient. The D8 method gives straight lines following grid lines. MS has dependence from a broad area, illustrating strikingly the problems with MS, even for a simple surface. The dependence map for *Lea*'s [1992] method is a stair step path roughly perpendicular to the

contours, as expected. DEMON is similar with some spillover into adjacent pixels due to the two-dimensional flow representation. D∞ has dependence from a narrower band 45° wide upslope of the point under consideration. The axis of this band is perpendicular to the contours.

For each of these example surfaces, cone, inward cone, and plane, the true upslope area was computed at each grid point and compared to results from each of the DEM procedures. Table 2 presents the differences between the theoretical result and each DEM procedure.

In evaluating the error statistics the grid direction bias introduced by D8, clearly evident in the figures, is responsible for the large mean square error (MSE) on the cone surfaces. Curiously, D8 does well for the plane because the area is the same whether one counts along the grid or perpendicular to contours. This would not have been the case had the ridge not been aligned with the grid. *Quinn et al.*'s [1991] MS method does best for the inward cone where the concave surface limits

Table 2. Differences Between Theoretical and DEM-Computed Upslope Area for Test Examples Expressed in Terms of the Mean Error and Mean Square Error

	Outward Cone		Inward Cone		Plane	
	Bias Mean $(A - \hat{A})$	MSE Mean $((A - \hat{A})^2)$	Bias Mean $(A - \hat{A})$	MSE Mean $((A - \hat{A})^2)$	Bias Mean $(A - \hat{A})$	MSE Mean $((A - \hat{A})^2)$
D8	−0.13	2.13	1.76	118.88	−0.17	0.065
MS	−0.81	0.69	−1.07	5.70	−1.37	2.065
Lea's [1992] method	−1.29	2.41	−4.05	44.00	−2.57	7.912
DEMON	−0.37	0.17	−0.37	19.23	−0.40	0.161
D∞	−0.13	0.20	1.87	30.58	−0.17	0.065

Bias, mean error; MSE, mean square error; A, true upslope area; $\hat{A}$, computed upslope area.
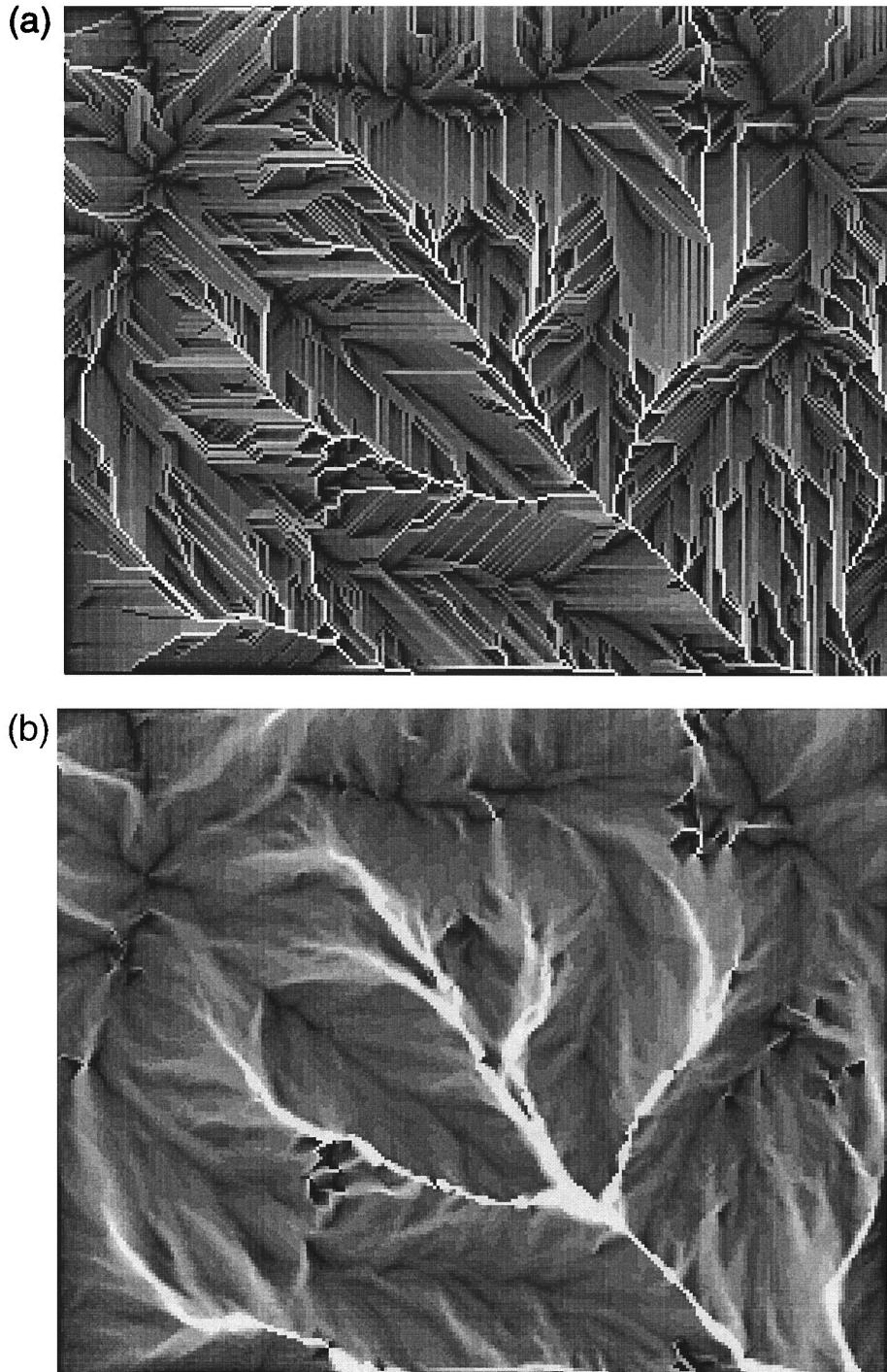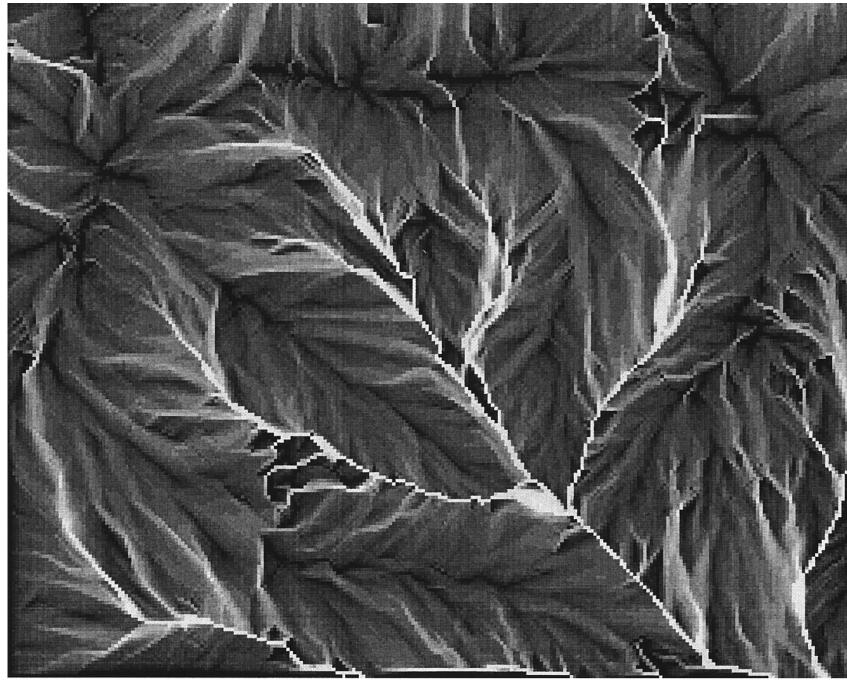
Figure 9. Images of upslope area for a portion of the Tennessee Valley study area DEM, Marin County, California. A logarithmic scale of gray shades is used with lighter shades corresponding to higher values. This is a 2-m resolution DEM generated from low-altitude stereo aerial photographs [*Dietrich et al.*, 1992, 1993; *Montgomery and Foufoula-Georgiou*, 1993]. (a) Single-direction, D8, procedure; (b) *Quinn et al.* [1991] procedure, MS; and (c) new procedure, D∞.

dispersion. However, it does poorly for the plane and outward cone owing to its substantial lateral dispersion. For example, with the outward cone, MS pixels along the outward edge have a component of slope parallel to the edge towards the corners. Therefore some fraction of flow that should exit the domain at the center is directed towards the corners, increasing the sum of upslope area around the edge above the area of the domain. *Lea*'s [1992] method in all cases has large MSE and bias due to

a bias toward overestimating upslope area by counting a contribution of 1 even if a flow path from a pixel only just crosses the corner of a pixel. In terms of statistics DEMON and D∞ are quite competitive. Both have small MSE and bias for the outward cone and plane and small MSE relative to Lea's and D8 for the inward cone. DEMON is better on the inward cone. This is due to the continuity across pixels maintained by DEMON with its flow tube procedure. Toward the middle of the

(c)

Figure 9. (continued)
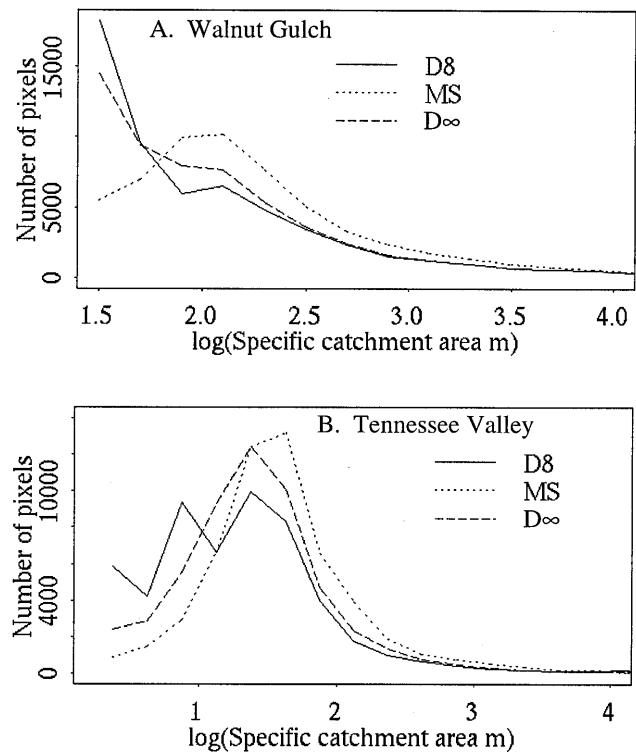
cone DEMON has many flow tubes at spacing much finer than the cell size. D∞ mixes the flow in each cell resulting in some blockiness evident in Figure 6e. Though informative, these statistics do not provide the complete picture. The good performance of MS on the inward cone is due to its dispersion being contained and considerable concentric averaging smoothing grid effects that are not so smoothed by the other methods. However, this averaging which contributes to small error statistics for a symmetric test case is in general undesirable as it results in loss of resolution.

Figure 8 shows the upslope area for portion of the Walnut Gulch Experimental Watershed calculated using D8, MS, and D∞. This is a 30-m resolution DEM from the U.S. Geological Survey Hay Mountain and Tombstone 7.5-min quadrangles. The differences at this scale are quite subtle, but it is possible to see more streakiness associated with the grid from the D8 procedure (Figure 8a) than with that from MS (Figure 8b) and D∞ (Figure 8c).

Figure 9 shows the upslope area for a portion of the Tennessee Valley area near San Francisco, California. This is a high-resolution (2-m grid) DEM generated from low-altitude stereo aerial photographs [*Dietrich et al.*, 1992, 1993; *Montgomery and Foufoula-Georgiou*, 1993]. At this scale the differences are much more noticeable than was the case for Figure 8. The D8 procedure results in streaks aligned with the grid indicating that flow down hillsides is biased by the grid alignment. The D∞ and MS procedures do not suffer from these problems. The D∞ results seem to have more sharpness than MS. This is due to less grid dispersion. Upslope areas were not computed with DEMON or *Lea*'s [1992] method for the real DEMs, because in the case of Lea's method it performed poorly in the test example evaluation (Table 2), and the DEMON code does not work automatically given the flat areas and situations requiring exceptions present in this data. The DEMON downslope code identified 6607 sinks in the Walnut Gulch DEM, even after the pits had been filled.

In Figure 10, histograms showing the distribution of specific

catchment area by the methods D8, MS, and D∞ are shown. These indicate significant differences in the number of pixels computed to have a certain specific catchment area at the low end of the specific catchment area scale. At the high end the methods all give similar results. Specific catchment area is


Figure 10. Histograms indicating the distribution of specific catchment area by each method. (a) Portion of Walnut Gulch Watershed shown in Figure 8. (b) Portion of Tennessee Valley area shown in Figure 9.

small on hillslopes and large in valleys and on the channel networks. Therefore, if the intent is demarcation of valleys or channels, for example, using the notion of a critical support area, the different methods will give similar results. However, if the intent is to use the specific catchment areas for distributed modeling of hydrologic processes, such as runoff generation or erosion, then the different methods will give differing results.

Conclusions

A new procedure for the representation of flow directions and the calculation of upslope area using grid-based digital elevation models was presented. The procedure is based on representing flow direction as a single angle taken as the steepest downward slope on the eight triangular facets centered at each pixel. Results from the procedure were compared to other grid-based procedures for calculation of upslope area from grid DEMs, using test examples and low- and high-resolution DEM data. On the basis of the evaluation of test statistics and examination of influence and dependence maps, the new procedure performs better than D8, *Lea*'s [1992] method, and MS and is comparable to DEMON [*Costa-Cabral and Burges*, 1994]. The new procedure overcomes the problems of loops and inconsistencies that plague plane-fitting methods such as DEMON. In real DEMs, significant differences between the distribution of specific catchment area were obtained depending on the method used. Differences are more marked as digital elevation data resolution increases, especially at hillslope scales. Where results from the different methods differ, the choice of methods becomes important, and this paper has argued that the new method presented provides a simple effective approach that should warrant consideration.

Availability

Software that implements these procedures is available electronically on the INTERNET from the author (dtarb@cc.usu.edu, http://www.engineering.usu.edu/dtarb/) and anonymous ftp from fox.cee.usu.edu.

References

Band, L. E., Topographic partition of watersheds with digital elevation models, *Water Resour. Res.*, *22*(1), 15–24, 1986.

Beven, K. J., and M. J. Kirkby, A physically based variable contributing area model of basin hydrology, *Hydrol. Sci. Bull.*, *24*(1), 43–69, 1979.

Beven, K., M. J. Kirkby, N. Schofield, and A. F. Tagg, Testing a physically based flood forcasting model (TOPMODEL) for three UK catchments, *J. Hydrol.*, *69*, 119–143, 1984.

Costa-Cabral, M., and S. J. Burges, Digital elevation model networks (DEMON): A model of flow over hillslopes for computation of contributing and dispersal areas, *Water Resour. Res.*, *30*(6), 1681–1692, 1994.

Dietrich, W. E., C. J. Wilson, D. R. Montgomery, J. McKean, and R. Bauer, Erosion thresholds and land surface morphology, *Geology*, *20*, 675–679, 1992.

Dietrich, W. E., C. J. Wilson, D. R. Montgomery, and J. McKean, Analysis of erosion thresholds, channel networks, and landscape morphology using a digital terrain model, *J. Geol.*, *101*, 259–278, 1993.

Fairfield, J., and P. Leymarie, Drainage networks from grid digital elevation models, *Water Resour. Res.*, *27*(5), 709–717, 1991.

Freeman, T. G., Calculating catchment area with divergent flow based on a regular grid, *Comput. Geosci.*, *17*(3), 413–422, 1991.

Jenson, S. K., Applications of hydrologic information automatically extracted from digital elevation models, *Hydrol. Process.*, *5*(1), 31–44, 1991.

Jenson, S. K., and J. O. Domingue, Extracting topographic structure from digital elevation data for geographic information system analysis, *Photogramm. Eng. Remote Sens.*, *54*(11), 1593–1600, 1988.

Lammers, R. B., and L. E. Band, Automating object representation of drainage basins, *Comput. Geosci.*, *16*(6), 787–810, 1990.

Lea, N. L., An aspect driven kinematic routing algorithm, in *Overland Flow: Hydraulics and Erosion Mechanics*, edited by A. J. Parsons and A. D. Abrahams, Chapman & Hall, New York, 1992.

Mark, D. M., Network models in geomorphology, in *Modelling in Geomorphological Systems*, chap. 4, edited by M. G. Anderson, pp. 73–97, John Wiley, New York, 1988.

Marks, D., J. Dozier, and J. Frew, Automated basin delineation from digital elevation data, *Geo. Processing*, *2*, 299–311, 1984.

Martz, L. W., and J. Garbrecht, Numerical definition of drainage network and subcatchment areas from digital elevation models, *Comput. Geosci.*, *18*(6), 747–761, 1992.

Montgomery, D. R., and W. E. Dietrich, A physically based model for the topographic control on shallow landsliding, *Water Resour. Res.*, *30*(4), 1153–1171, 1994.

Montgomery, D. R., and E. Foufoula-Georgiou, Channel network source representation using digital elevation models, *Water Resour. Res.*, *29*(12), 3925–3934, 1993.

Moore, I. D., R. B. Grayson, and A. R. Ladson, Digital terrain modelling: A review of hydrological, geomorphological, and biological applications, *Hydrol. Process.*, *5*(1), 3–30, 1991.

Morris, D. G., and R. G. Heerdegen, Automatically drained catchment boundaries and channel networks and their hydrological applications, *Geomophology*, *1*, 131–141, 1988.

O'Callaghan, J. F., and D. M. Mark, The extraction of drainage networks from digital elevation data, *Comput. Vision Graphics Image Process.*, *28*, 328–344, 1984.

Quinn, P., K. Beven, P. Chevallier, and O. Planchon, The prediction of hillslope flow paths for distributed hydrological modeling using digital terrain models, *Hydrol. Proc.*, *5*, 59–80, 1991.

Quinn, P. F., K. J. Beven, and R. Lamb, The ln (a/tan β) index: How to calculate it and how to use it within the Topmodel framework, *Hydrol. Process.*, *9*, 161–182, 1995.

Tarboton, D. G., The analysis of river basins and channel networks using digital terrain data, Sc.D. thesis, Dep. of Civ. Eng., Mass. Inst. of Technol., Cambridge, 1989. (Also available as *Tech. Rep. 326*, Ralph M. Parsons Lab. for Water Resour. and Hydrodyn., Dep. of Civ. Eng., Mass. Inst. of Technol., Cambridge, 1989).

Tarboton, D. G., R. L. Bras, and I. Rodriguez-Iturbe, The fractal nature of river networks, *Water Resour. Res.*, *24*(8), 1317–1322, 1988.

Tarboton, D. G., R. L. Bras, and I. Rodriguez-Iturbe, On the extraction of channel networks from digital elevation data, *Hydrol. Process.*, *5*(1), 81–100, 1991.

Tarboton, D. G., R. L. Bras, and I. Rodriguez-Iturbe, A physical basis for drainage density, *Geomorphology*, *5*(1/2), 59–76, 1992.

Wolock, D. M., and G. J. McCabe, Comparison of single and multiple flow direction algorithms for computing topographic parameters, *Water Resour. Res.*, *31*(5), 1315–1324, 1995.

Wood, E., F. M. Sivapalan, and K. Beven, Similarity and scale in catchment storm response, *Rev. Geophys.*, *28*(1), 1–18, 1990.

Wu, W., Distributed slope stability analysis in steep, forested basins, Ph.D. thesis, Watershed Sci., Utah State Univ., Logan, 1993.

Zhang, W., and D. R. Montgomery, Digital elevation model grid size, landscape representation, and hydrologic simulations, *Water Resour. Res.*, *30*(4), 1019–1028, 1994.

D. G. Tarboton, Department of Civil and Environmental Engineering, Utah State University, Logan, UT 84322-4110. (e-mail: dtarb@cc.usu.edu)